REPORT DOCUMENTATION PAGE

Form Approved OMB No. 0704-0188

Public reporting burden for this collection of information is estimated to average 1 hour per response, including the time for reviewing instructions, searching existing data sources, gathering and maintaining the data needed, and completing and reviewing the collection of information. Send comments regarding this burden estimate or any other aspect of this collection of information, including suggestions for reducing the burden, to Department of Defense, Washington Headquarters Services, Directorate for Information Operations and Reports (0704-0188), 1215 Jefferson Davis Highway, Suite 1204, Arlington, VA 22202-4302. Respondents should be aware that notwithstanding any other provision of law, no person shall be subject to any penalty for failing to comply with a collection of information if it does not display a currently valid OMB control number. **PLEASE DO NOT RETURN YOUR FORM TO THE ABOVE ADDRESS.**

1. REPORT DATE *(DD-MM-YYYY)* 20-09-2007	2. REPORT TYPE Final Report	3. DATES COVERED *(From – To)* 1 July 2006 - 26-Jun-08

4. TITLE AND SUBTITLE	5a. CONTRACT NUMBER
Mechanisms of microdamage development in laminated composites in thermo-mechanical fatigue	FA8655-06-1-3001
	5b. GRANT NUMBER
	5c. PROGRAM ELEMENT NUMBER

6. AUTHOR(S)	5d. PROJECT NUMBER
Professor Janis Varna	5d. TASK NUMBER
	5e. WORK UNIT NUMBER

7. PERFORMING ORGANIZATION NAME(S) AND ADDRESS(ES) Lulea University of Technology LULEA SE 971 87 SWEDEN	8. PERFORMING ORGANIZATION REPORT NUMBER N/A

9. SPONSORING/MONITORING AGENCY NAME(S) AND ADDRESS(ES) EOARD Unit 4515 BOX 14 APO AE 09421	10. SPONSOR/MONITOR'S ACRONYM(S)
	11. SPONSOR/MONITOR'S REPORT NUMBER(S) Grant 06-3001

12. DISTRIBUTION/AVAILABILITY STATEMENT

Approved for public release; distribution is unlimited.

13. SUPPLEMENTARY NOTES

14. ABSTRACT

This report results from a contract tasking Lulea University of Technology as follows: The objectives of the proposed research project are (a) to reveal the mechanisms of damage initiation and damage propagation in thermo-mechanical fatigue and to identify governing parameters, (b) to describe the evolution of the actual damage modes by evolution laws, and (c) to develop efficient methodology for parameter identification in the evolution laws. We expect that the proposed research will lead to deeper fundamental understanding of the observed trends in thermal fatigue, development of predictive tool to describe composites degradation in thermal fatigue, cost savings due to 'smart' testing based on the accumulated knowledge, and structures with improved resistance to thermal cracking will be designed.

15. SUBJECT TERMS
EOARD, Fracture mechanics, Environmental Testing, Composites, Damage Assessment

16. SECURITY CLASSIFICATION OF:			17. LIMITATION OF ABSTRACT UL	18, NUMBER OF PAGES	19a. NAME OF RESPONSIBLE PERSON WYNN SANDERS, Maj, USAF
a. REPORT UNCLAS	b. ABSTRACT UNCLAS	c. THIS PAGE UNCLAS		26	19b. TELEPHONE NUMBER *(Include area code)* +44 (0)1895 616 007

Standard Form 298 (Rev. 8/98)
Prescribed by ANSI Std. Z39-18

Mechanisms of microdamage development in laminated composites in thermo-mechanical fatigue

Professor Janis Varna
Luleå University of Technology,
Luleå, Se 97187 Sweden
Janis.Varna@ltu.se

Content

Summary

This report is a continuation of the work described in the 6 month report regarding the stitch crack formation. New results are presented concerning the local stress concentrations at the tip of an existing intralaminar crack responsible for stitch crack formation in adjacent layer. Analysis was performed using FEM in generalized plane strain formulation.

The attempts to improve the stress distribution (reduce stress concentrations) by changing the geometrical parameters of layers was not successful: the stress concentration shape was not changing significantly.

An introduction of an inter-layer with fiber orientation transverse to the fiber orientation in the layer with intralaminar cracks is a possible solution: a) stitch cracks in the inter-layer do not form because of the fiber orientation; b) the stress concentration is localized in the inter-layer only. This conclusion holds also for rather thin interlayer with a thickness = 0.25 of a regular prepreg layer thickness.

Fatigue data for intralaminar cracking available in literature are analysed and possible reasons for observed discrepancies are discussed. Based on this analysis statistical model for crack initiation in thermo-mechanical fatigue is suggested. It can be considered as a generalization of the Weibull's strength distribution model to fatigue case. Fatigue effects in the distribution are included by considering the defect distribution development with time and stress. Methodology for testing to validate the model and to determine the involved material parameters is described.

List of used symbols

x, y - axial and out-of-plane coordinates

T -temperature difference

$\sigma_{x0}^{90}, \sigma_{x0}^{0}$ - stresses in 90-layer and 0-layer

$2L_0$ -crack spacing

$E_1, E_2, \nu_{12}, G_{12}, \nu_{23}, G_{23}, \alpha_1, \alpha_2$ - ply thermo-elastic properties

α_x thermal expansion coefficient in x-direction

t_k -thickness of the k-th layer

G -strain energy release rate

N -number of cycles in fatigue

N_{in} number of cycles for initiation

$\Delta\varepsilon$ strain range in fatigue

1. Introduction

Microcracks initiate and grow in laminates subjected to thermo-mechanical loading. The first damage modes are matrix and interface related cracks with a crack plane transverse to the laminate midplane. They usually cover the whole layer thickness and grow in the direction parallel to the fiber orientation in the ply. In Fig.1.1 a transverse crack in the surface layer as well as a transverse crack in the internal layer is shown. These cracks are called in following primary cracks because their initiation and growth is related only to the defects/ cracks in the considered layer.
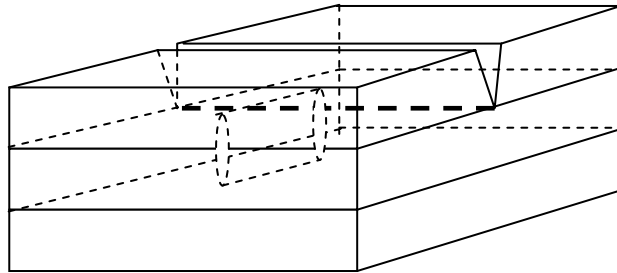
a) transverse cracks in surface layer and in an internal layer
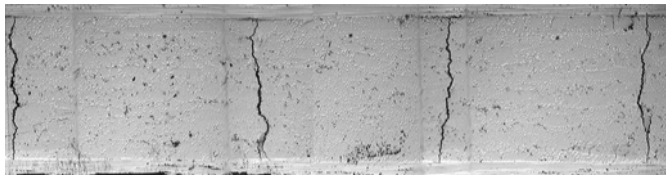
b) micrograph showing a system of transverse layers in a thick 90-layer

Figure 1.1 First damage mode in laminates: matrix crack in layers

Large stress concentrations at the tip of the transverse crack initiate secondary damage modes: local interface delamination (see Fig. 1.1a) and stitch crack formation in adjacent off-axis layers, see Fig.1.2. Stitch cracks are primarily caused by the concentration of stress components transverse to the crack plane. As shown using FEM in the first report of this project, these high local stress components are much larger than other stresses and their projection/transformation to direction transverse to fibers in the adjacent layer leads to tensile transverse stresses which can initiate small matrix cracks there which grow with the number of cycles or increasing loading.
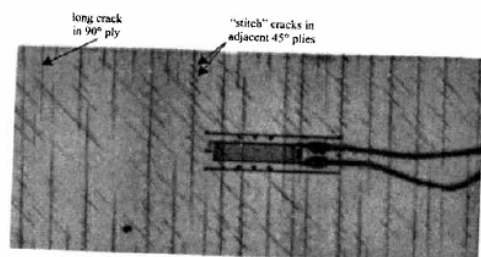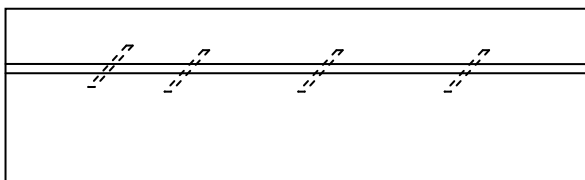

Fig. 12. X-ray showing stitch cracks in a $[0/45_2/90]_s$ laminate (Yokozek et al. [29]).

Figure 1.2. Stitch cracks in adjacent off-axis layer initiated by a large transverse crack. A) Schematic view from the top of the laminate; B) micrograph [1]

Stitch cracks do not develop in the adjacent layer if its orientation is 90-degrees with respect to the layer with cracks. In this particular case the stress concentration is in the fiber direction of the adjacent layer and because of that it would cause some fiber breaks (in mechanical tensile loading) but the appearance of matrix cracks is highly unlikely.

The general features of the stress field at the transverse crack tip were described in Report 1 of this project. Semi-empirical expressions approximating the shape of the stress distributions as dependent on the anisotropic elastic constants and laminate lay-up were presented. Also an analytical stress distribution model was developed. This information will be useful for development of approximate initiation and evolution models for stitch cracks in this region.

 The Chapter 2 of the present report contains further investigation results on this subject using FEM. Different combinations of layer thicknesses were analysed to find the possibly best combination. The main emphasis was on possible reduction of the stress concentrations in layer by introducing thin 90-degree oriented inter-layers between the layer with transverse cracks and the next layer. This inter-layer would "absorb" the stress concentrations but would not be damaged. Then the stitch crack initiation in off-axis layers would be suppressed.

In Chapter 3 the available criteria for matrix crack initiation in fatigue are analyzed and a possible approach for the analysis and predictions is outlined. The method for fatigue crack growth initiation is based on Weibull type of strength distribution in which fatigue effects are incorporated.

2. Stress concentrations at the transverse crack tip

2.1 The effect of layer thicknesses on stress concentration at the tip of a transverse crack in 90-layer

The objective of this sub-task was to study the effect of the layer relative thickness on the values and the zone size of the local stress concentrations caused by the presence of transverse crack in one layer with the aim to find the best combination (if possible). The coordinate system is chosen so, that the cracked layer is a 90-layer. The considered laminate configurations are shown in Fig.2.1 It roughly represents [0,45,90]s laminate. The thermal loading was achieved by applying temperature difference -100C.
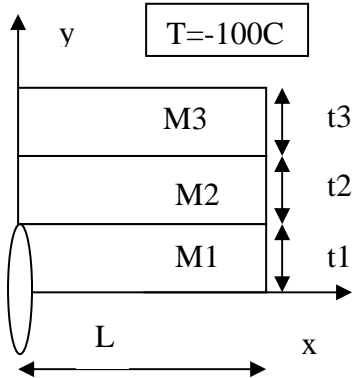

Figure 2.1 ¼ of the laminate repeating element with a crack in the central layer.

The used material properties are given in Table 2.1 and 2.2. The Material M1 represents the 90-layer, material M3 represents 0-layer and material M2 approximately represents the effective properties of 45 layer in x,y coordinates (not calculated, just assumed). The half-distance between cracks $L_0 =5$ (non-interactive cracks).

Table 2.1 Elastic properties of used materials

Material	Ex (GPa)	Ey (GPa)	Ez (GPa)	Nxy	ν_{xz}	ν_{yz}	Gxy (GPa)	Gxz (GPa)	Gyz (GPa)
M1	10	10	150	0.4	0.3*10/150	0.3*10/150	Isotr.	5	5
M2	50	10	50	0.3	0.3	0.3	5	5	5
M3	150	10	10	0.3	0.3	0.4	5	5	5

Table 2 2 Thermal expansion coefficients

Material	α_x (10^{-6})	α_y (10^{-6})	α_z (10^{-6})
M1	20	20	5
M2	5	20	5
M3	5	20	20

The considered geometrical cases are given in Table 2.3

Table 2.3   Geometrical configurations and used notation for cases

Case	t1	t2	t3
$t_{90}=1,t_{45}=1$	1	1	0
$t_{90}=1,t_{45}=1,t_0=1$	1	1	1
$t_{90}=1,t_{45}=1,t_0=2$	1	1	2
$t_{90}=1,t_{45}=1,t_0=0.5$	1	1	0.5
$t_{90}=1,t_{45}=0.5,t_0=1$	1	0.5	1
$t_{90}=1,t_{45}=0.5,t_0=2$	1	0.5	2

The stress distribution problem is solved using ANSYS in generalized plane strain formulation. Results are in Fig 2.2 and Fig. 2.3. X-axis tresses are shown only in the layer adjacent to the cracked 90-layer.

The stress profiles in Fig.2.2 are rather similar, except the curve where the 45 –layer was NOT supported by 0-layer on the top. Otherwise changing the thickness of the top 0-layer does not affect the local stress concentration in the 45-layer at the transverse cracks tip. The absence of the 0-layer change the stress concentration curve but it is basically because of dramatic change in the laminate theory thermal stress state in this layer due to absence of the 0-layer (in this case the 45-layer is much more compressed because it alone (without help from the 0-layer) has to resist the " shrinking trends" of the 90-layer.

In Fig. 2.3 The stress distribution in the 45-layer with thickness 1 and $t_0=1$ is compared with solution for laminates where that 45-layer thickness is only 0.5. Results for two different thicknesses of the supporting 0-layer are presented. All three curves almost coincide that prove that neither the adjacent 45-layer thickness nor the thickness of the next layer can be used to optimize the laminate with respect to the local stress concentrations caused by primary cracks.
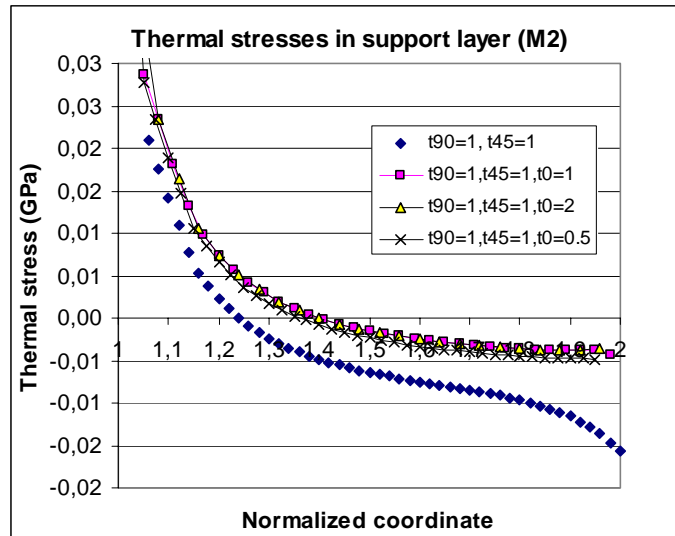
Figure 2.2 Stress distribution in y-direction across the layer with material M2 in the crack tip cross section.
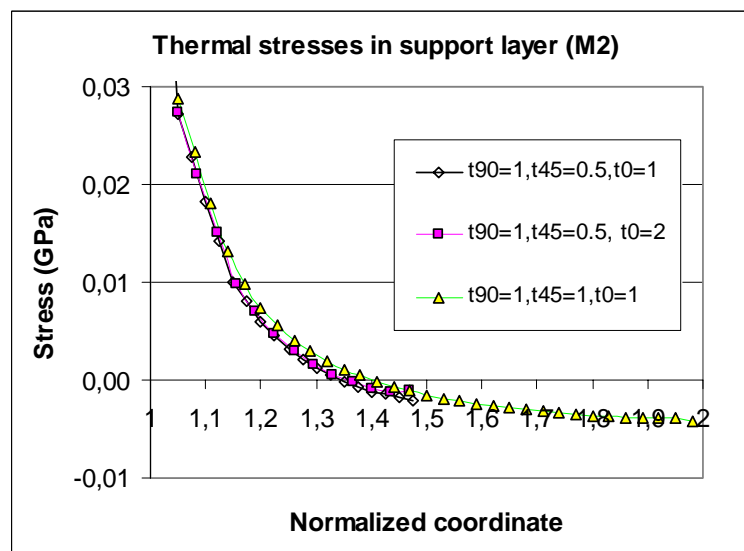

Figure 2.3 The same as in Fig.2.2 but for different geometries.

Results show that only the case when the 45 - layer (M2-layer) is also the outer layer is different.

The following notes has to be made regarding the generality of the results presented in this sub-section

1. Analysis was done with arbitrary chosen properties. Just by coincidence α in M2 and M3 in x-direction are equal. One could choose properties better by using proper properties transformation.
2. The upper layer M3 has 0-layer properties. Most probably in the real laminate configuration the next will be -45-layer. However, if we could not get any positive effect from 0-layer it is difficult to expect it from another 45 layer.

2.2 The effect of special inter-layer introduced to reduce stress concentration in the 45 layer in the vicinity of a primary transverse crack

A special inter-layer with orientation of 90-degrees with respect to the orientation of layer with primary cracks was introduced between the layer with primary cracks and the following 45-layer where stitch cracks are usually prone to form. It was expected that most of the stress concentration will be in this layer and in this way we can avoid stitch crack formation in the 45-layer.

The temperature difference is taken -100C. Thermo-elastic properties of the UD composite are in given in Tables 2.4 and 2.5. Properties of 45 layer were calculated using CLT for [45,-45]s laminate (this is the way how the 45 layer will behave in the laminate.

Table 2.4 Elastic properties of the UD composite materials

Material	Ex (GPa)	Ey (GPa)	Ez (GPa)	ν_{xy}	ν_{xz}	ν_{yz}	Gxy (GPa)	Gxz (GPa)	Gyz (GPa)
0-layer	150	10	10	0.3	0.3	0.4	5	5	5

Table 2.5 Thermal expansion coefficients

Material	$\alpha_x (10^{-6})$	$\alpha_y (10^{-6})$	$\alpha_z (10^{-6})$
M3	5	20	20

Case A

If the original laminate is [0,45,-45,90]s and the crack is in the 90-layer, we introduce an additional inter-layer with 0- orientation and with thickness 0.5 and the laminate becomes [0,45,-45,0_{0.5},90]s. It was decided that the efficiency to reduce the local stress concentration in this case can be studied on laminate [45,0 _{0.5},90]s with crack in 90 –layer. This laminate in contrast to the used in practice is not balanced and therefore an additional constraint to its macroscopic rotation was applied. The reason for this simplification, which usefulness will be discussed at the end of this report, was to make analysis simpler.

The considered simplified laminate configuration is shown in Fig.2.4. The objective is to analyze the stress in the 0-inter-layer and in the following 45 layer which should be protected from stress concentrations
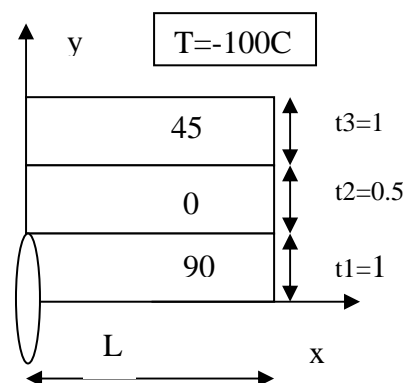

Figure 2.4 ¼ of the laminate repeating element with a crack in the central layer.

This problem is solved using ANSYS in generalized plane strain formulation .

The calculated stress distributions shown in Fig 2.6 may be compared with Fig. 2.7 where the solution obtained for [0,45,90]s laminate (without the special inter- layer) with crack in 90 layer as shown in Fig 2.5. The solution for this configuration was given in the Section 2.1 but it is not directly applicable for comparison because the 45-layer properties there were not calculated, they were assumed. This time the properties were calculated using properties in Table 2.4 and 2.5.
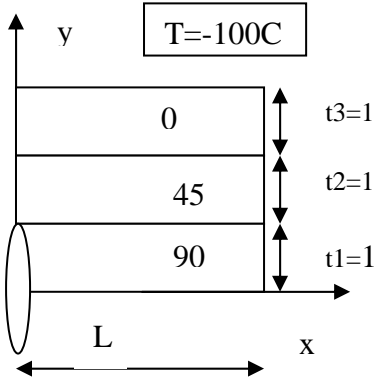
Figure 2.5   ¼ of the [0,45,90]s laminate repeating element with a crack in the central layer.
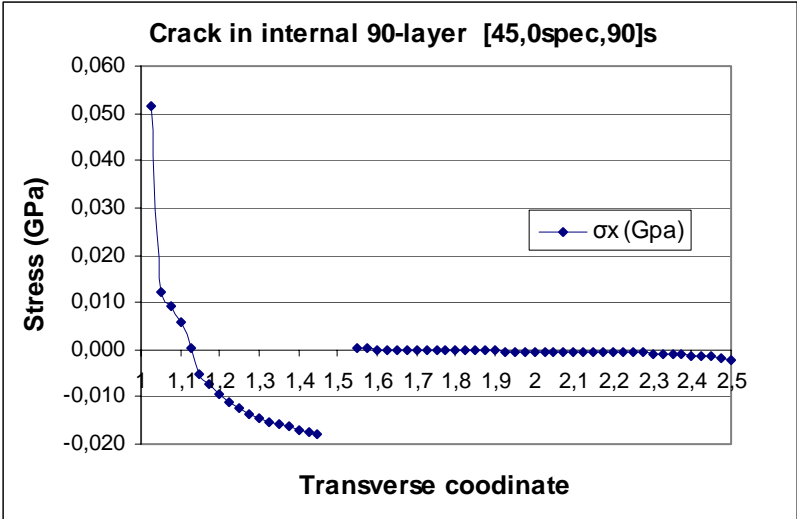
Figure 2.6 Thermal stress x-axis stress distribution in y-direction across the special 0-layer $y \in [1,1.5]$ and the 45 layer $y \in [1.5,2,5]$.
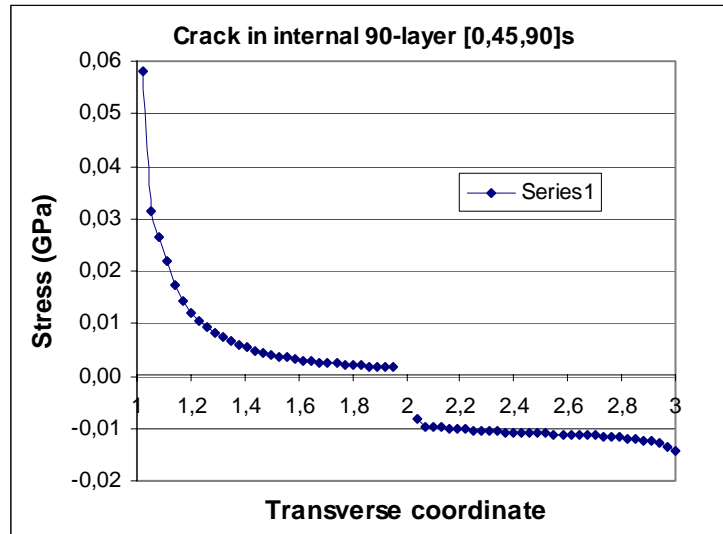
Figure 2.7   Thermal x-axis stress distribution in y-direction across the 45-layer $y \in [1,2]$ and in the 0 layer $y \in [2,3]$.

Following rather obvious conclusions can be obtained
- the stress concentration is only in the introduced 0-inter-layer
- Stresses in the 45 layer now are very uniform and roughly correspond to the ply-discount type of the laminate theory solution (in the plan of the crack in the 90-layer the 90-layer stress is zero which corresponds to play-discount model assumptions)
- It is useless to compare the stress levels in Fig 2.6 and Fig. 2.7 because they are for different laminates under thermal loading. For example stress in 45-layer was positive in the laminate in Fig 2.5 and it becomes negative in Fig 2.4. In other words the CLT levels of stresses are very different.

Case B

Corresponds to the laminate [0,45,-45,90]s with the crack is in the surface 0-layer.
We can consider this laminate as [90,-45,45,0]s and then the crack is a 90-layer crack.
In this case we introduce a 0-layer with thickness 0.5 after the cracked 90-layer and the laminate becomes [90,0 $_{0.5}$,-45,-45,0]s.
Again, a simplified laminate was analyzed because it was decided that the efficiency to reduce the local stress concentration in this case can be studied on laminate [90,0 $_{0.5}$,45]s with crack in 90 –layer. The reason for this simplification was to make analysis simpler.
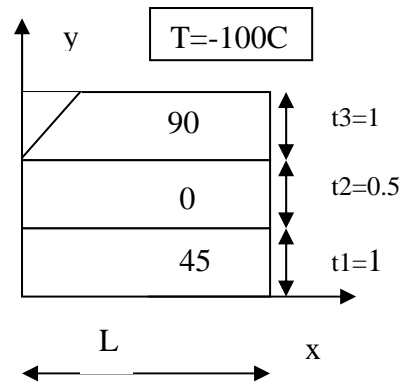
Figure 2.8 ¼ of the [90,0,45]s laminate repeating element with a crack in the central layer.

The considered laminate configuration are shown in Fig.5

The calculated x-axis stress profile is shown in Fig. 2.9 which demonstrates that the stress concentrations in the 45 layer are removed and the stress distribution is rather uniform
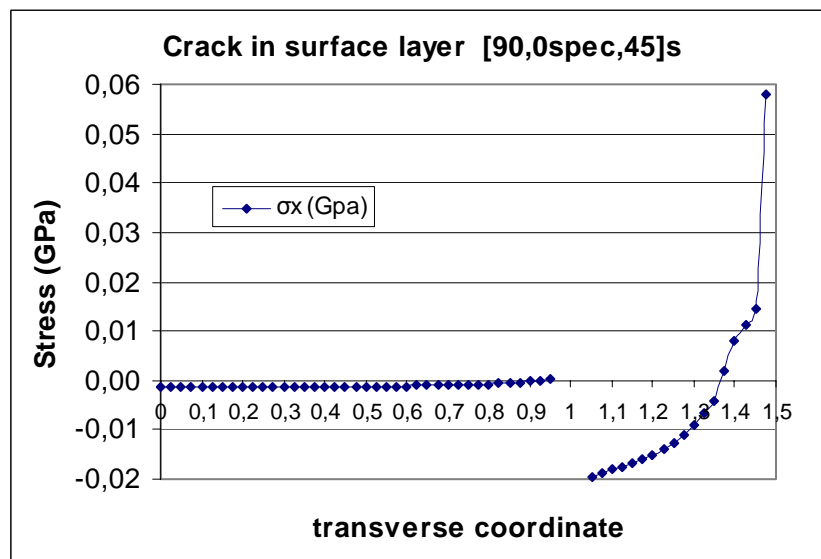

Figure 2.9 Thermal x-axis stress distribution in y-direction across the 45-layer $y \in [0,1]$ and in the special 0 layer $y \in [1,1.5]$ at the position of transverse crack in the surface layer.

The following conclusions follow from the results presented in this sub-section:
- Stress concentrations in 45-layer are removed in both cases
- More detailed comparison of the level of thermal stresses in the new laminate can be performed only analyzing the laminate real configuration including all layers

2.3 The effect of inter-layer on stress distribution in damaged [0,45,-45,90]s laminates

In this subsection the real lay-up [0,45,-45,90]s used in laminates is analyzed using material properties given in Tables 2.4 and 2.5. There are two possible positions to introduce the interlayer: a) after the surface 0- layer; b) between the middle 90-layer and the adjacent -45 layer.

In case a) analyzing thermal cracks in the surface layer it is convenient for discussion to rotate the laminate by 90-degrees obtaining a [90,45,-45,0]s laminate with cracks in 90-layer. The interlayer with orientation 0-degrees (of the same material) and with thickness 0.5 is introduced after the surface layer. In other words we have to compare the stress distributions in a 90-layer cracked [90,45,-45,0]s laminate and in a laminate $[90,0_{1/2},45,-45,0]$s laminate (also with cracks in the 90-layer. The stress state is compared on the cross-section corresponding to the continuation of the crack surface.

It can be seen from Fig. 2.10 that before introduction of the 0.5 thickness layer we have large stress concentrations in the 45 layer close to the cracked layer ($y \in [2;3]$). The stress distribution in this layer is with a large stress gradient and the concentration zone is not extending to the next layer.
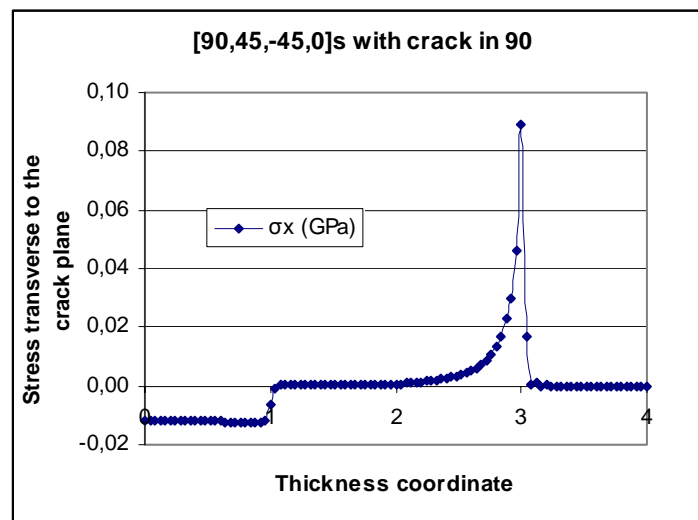

Fig 2.10 X-axis stress distribution over the thickness in the cracked laminate with configuration [90,45,-45,0]s

Introducing the 0-inter-layer the stress distribution change, see Fig.2.11, and all the zone of the stress concentration is inside of the 0-inter-layer in which stitch type modes of damage are not expected. The stress state in the 45 layer is uniformly distributed which indicates again that the stress state is not directly affected by the close crack tip. As mentioned above the constant value of the stress in this layer actually depends on the crack because the laminate theory solution in the crack plane is different than in the virgin laminate.

[90,0_0.5,45,-45,0]s withthin 0-layer
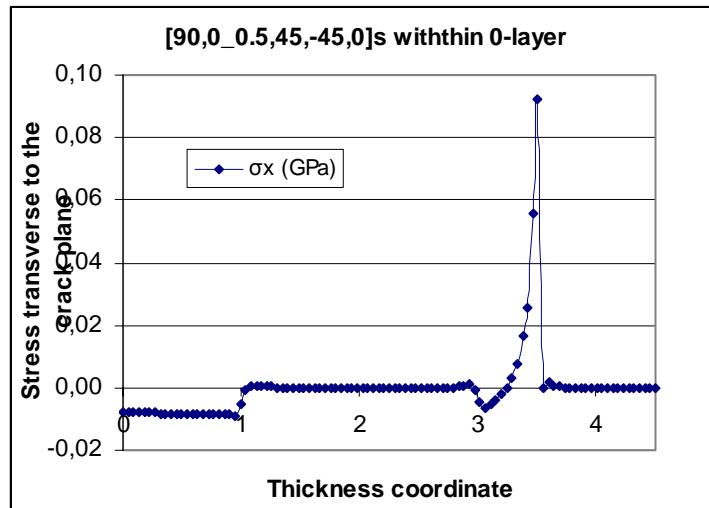
Figure 2.11 X-axis stress distribution over the thickness in the cracked modified laminate with configuration [90,0$_{1/2}$,45,-45,0]s

In the case b) the interlayer with 0-orientation and thickness 0.5 is introduced between the 90 layer and the -45 of the [0,45,-45,90]s laminate. The modified laminate has lay-up [0,45, -45,0$_{1/2}$,90]s.

The x-axis thermal stress distribution across the thickness of the [0,45,-45,90]s laminate is shown in Fig. 2.12. The stress on the crack surface ($y \in [0;1]$) is zero, there is a localized stress concentration zone in the next layer with -45 –orientation ($y \in [1;2]$). The stress state in the following layers is uniform and can be o9btained from laminate theory type of solutions.

[0,45,-45,90]s with crack in 90
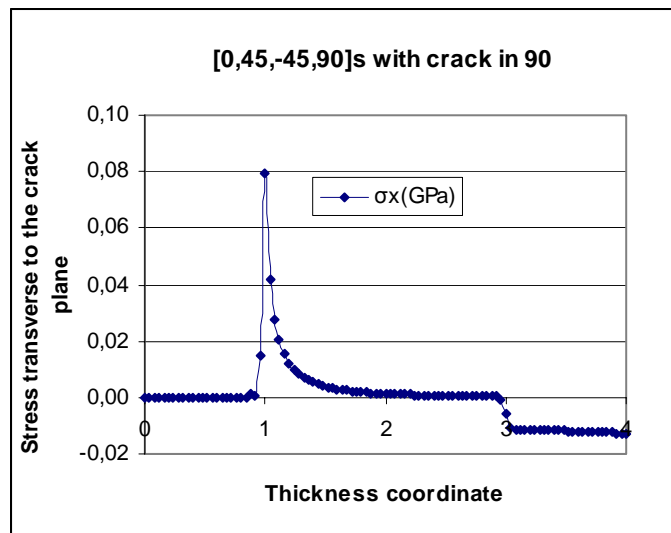
Fig 2.12 The x-axis thermal stress distribution in the [0,45,-45,90]s laminate with crack in 90-layer.

The stress distribution changes adding the inter-layer as described above see Fig. 2.13.

14

The stress concentration zone is now localized in the inter-layer with 0-orientation. The stress distribution in the rest of layers is uniform which indicates that they are outside the stress perturbation zone caused by the transverse crack in the 90-layer. The numerical values of these uniform stresses are slightly different than in the initial lay-up, which is the result of adding one more zero layer to the laminate.
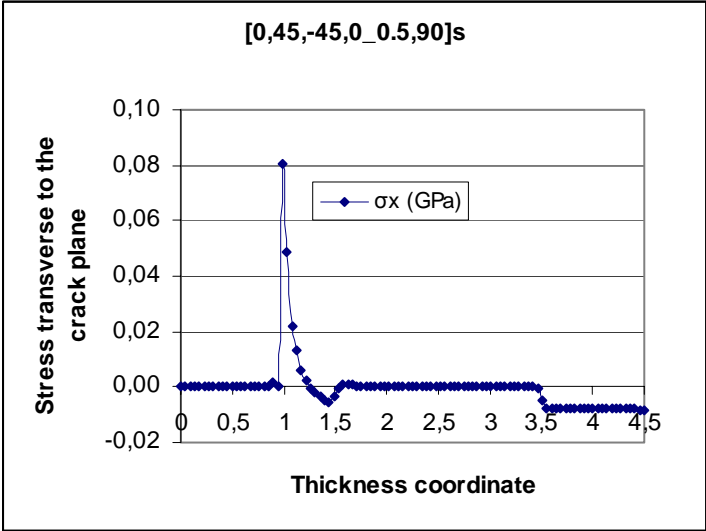

Figure 2.13 X-axis thermal stress distribution over the thickness in the modified laminate with configuration [0,45,-45, ,0$_{1/2}$,90]s and with cracks in the 90-layer.

2.4 The effect of a THIN inter-layer on stress distribution in damaged [0,45,-45,90]s laminates

In subsection 2.3 the analysis was performed for inter-layers with relative thickness 0.5 (as compared with the regular thickness of the prepreg layer). However, in experimental efforts the thickness is smaller: between 0.25 and 0.33 of the prepreg layer thickness.
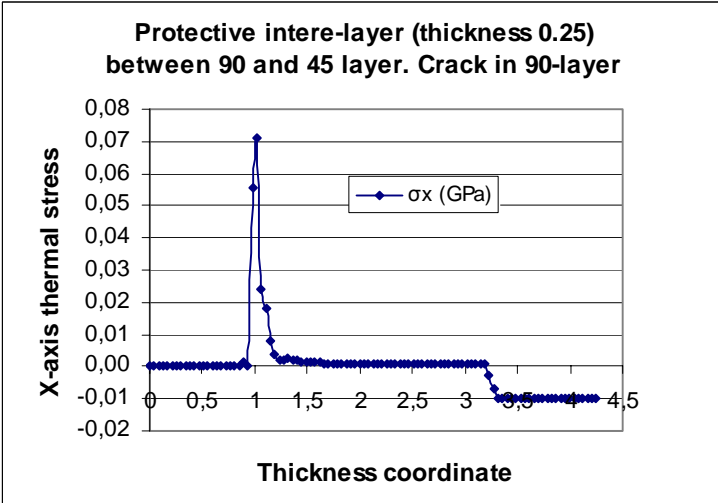
Figure 2.13 X-axis thermal stress distribution over the thickness in the modified laminate with configuration [0,45,-45, ,0$_{1/4}$,90]s and with cracks in the 90-layer.

Calculations were performed for inter-layer thickness 0.25.
The stress distribution across the laminate thickness in $[0,45,-45,,0_{1/4},90]s$ laminate is shown in Fig. 2.13. The stress concentration is localized in the inter-layer $y \in [1;1.25]$. Thermal stresses in other layers are uniform across the thickness.

The same conclusion follows from the stress distribution across the laminate thickness in $[90,0_{1/4},-45,45,0]s$ laminate is shown in Fig. 2.14: all the stress concentration is "absorbed" by the 0-inter-layer with thickness 0.25.
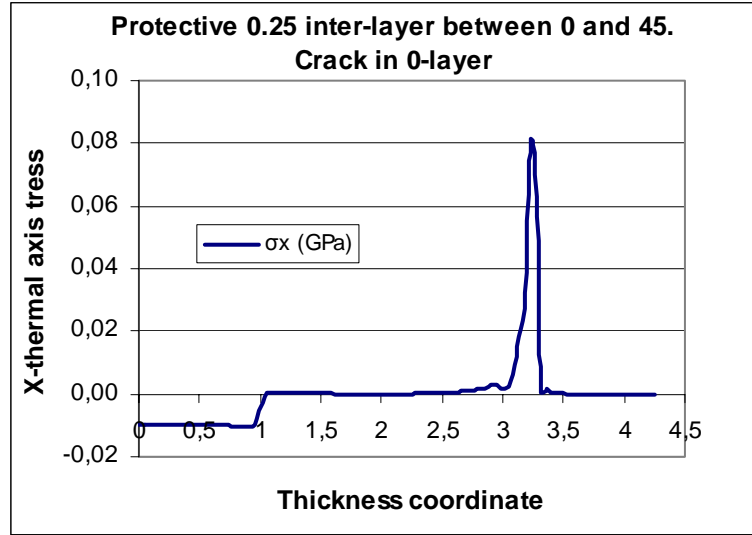
Figure 2.14 *X-axis stress distribution over the thickness in the cracked modified laminate with configuration $[90,0_{1/4},-45,45,0]s$.*

3. Criteria for matrix crack initiation in fatigue

3.1 Thermo-mechanical fatigue: experimental trends

It is well known that intralaminar (transverse) cracks develop in layers in thermo-mechanical fatigue loading, see x-ray micrographs of damaged cross-ply laminates in Fig. 3.1.
The current common opinion is that the propagation of these cracks can be described by Paris type of propagation law

$$\frac{dD}{dN} = A(\Delta G)^n \qquad \qquad \Delta G = G_{max} - G_{min} \qquad \qquad (1)$$

Here D is the damage state characterized by crack density, N is the number of fatigue cycles, A and n are material constants, G_{max} and G_{min} are the strain energy release rates corresponding to the highest and to the lowest value during the cycle. Theoretical stress distribution models are used to calculate the strain energy release rate.

(a) *n*=10   (b) *n*=40
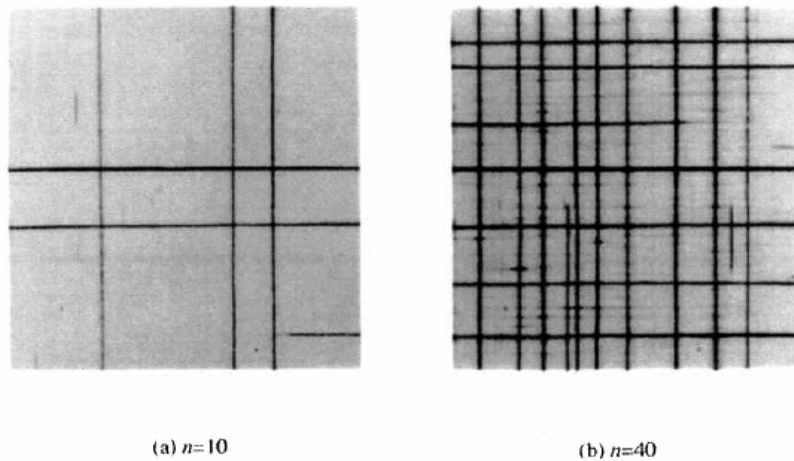
Figure 3.1   Transverse crak development in thermal fatigue (-196C to +250C) in AS4/PEEK [02,902]s laminates. From S. Kobayashi et all [2].

A convincing example of applicability of the Paris law was presented by Nairn [3] who performed mechanical fatigue tests on laminates with different lay-ups made of the same material, see Fig3.2

Figure 3.2: The microcrack density growth rate (in microcracks per mm per cycle) as a function of applied ΔG for Avimid® K Polymer/IM6 laminates. As indicated on the figure, the results are from three different cross-ply layups.
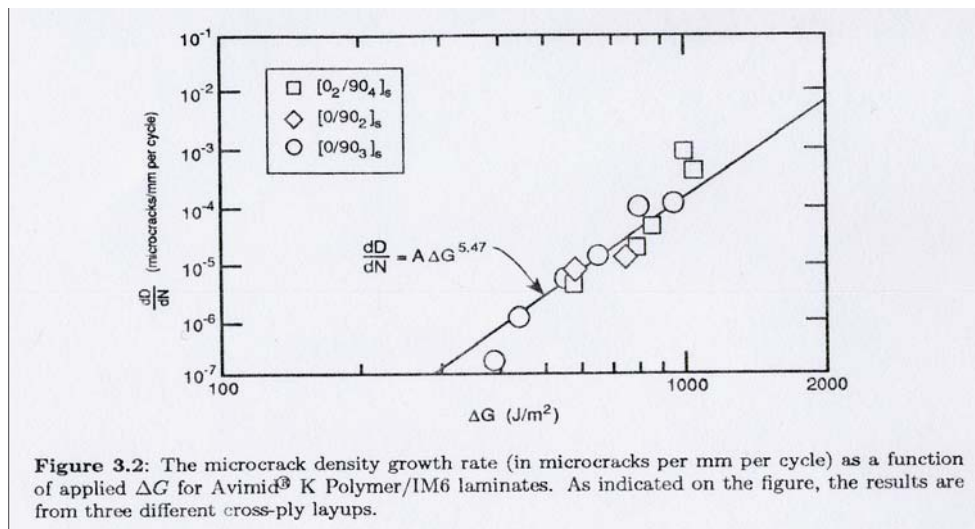
The damage growth rate is linear in the log-log axes and it is the same for all considered lay-ups.   The strain energy release rate was calculated using Hashin's variational stress distribution model with included thermal terms.

Similar mechanical fatigue tests performed by Takeda et al [4] on T800H/3631 [0,90m,0] laminates with m=4,8 and 12 lead to total failure of the modelling attempt using the Paris law, see Fig. 3.3

17
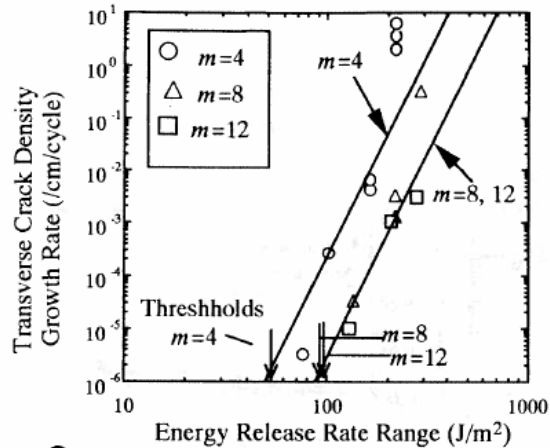
Figure 3.3 The crack density versus energy release rate curves in log-log axes [4]

The presented results for m=4 and m=8 do not lie on the same line. The slope in both cases in the Fig is shown the same , but it is definitely not the best fit to each data set separately. It appears that the constant A in (1) is not a material constant it depends on the laminate lay-up.

Several reasons may be responsible for this modelling failure: a) too simple stress analysis (however, the Hashin's analysis used in [3] is also simplified); b) large local delaminations which could affect the results (different stress state between cracks); c) unstable crack growth.

Also Nairn's [5] attempts to describe the thermal and mechanical fatigue by the same parameters in the Paris law were unsuccessful.
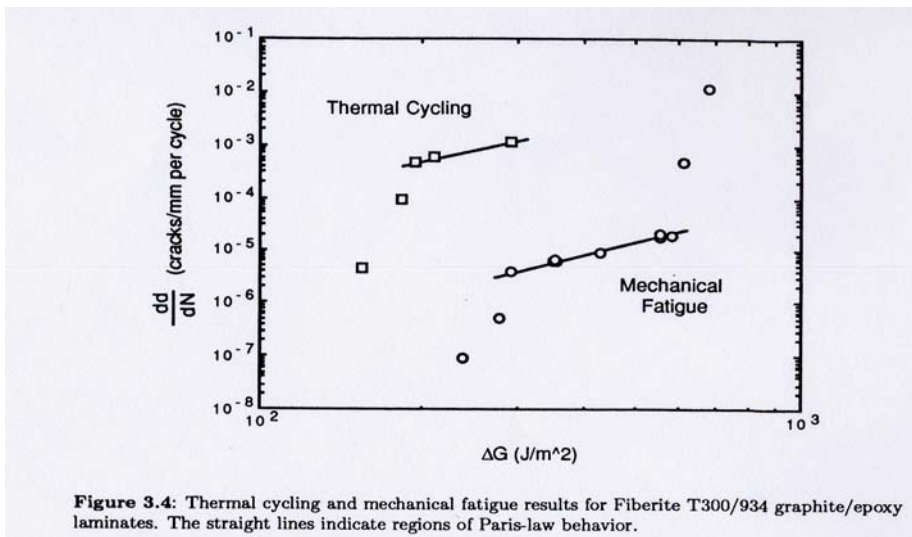
Figure 3.4: Thermal cycling and mechanical fatigue results for Fiberite T300/934 graphite/epoxy laminates. The straight lines indicate regions of Paris-law behavior.

Figure 3.4 Thermal cycling and mechanical fatigue results [5].

Results presented in Fig.3.4 convincingly demonstrate (the scale is logarithmic) that the "material" constants are absolutely different in thermal and mechanical fatigue. One of possible contributing factors may be general degradation of the material in thermal fatigue leading to reduced value of G_c. This idea was introduced by McManus, 1996 [6] and the dependence on the number of cycles was described by a power law. One could argue that G_c does not enter the Paris law equation (1). However, it may enter (1) through the

material constant A. In fact there exist several modifications of (1) where G_c is incorporated explicitly.

In 2001 Kobayashi [2] came to the same conclusion as Takeda: the Paris law is not applicable to his fatigue data, see Fig. 3.5. In thermal fatigue the damage growth rate with the strain energy release rate change is rather different even in different layers of the same laminate.
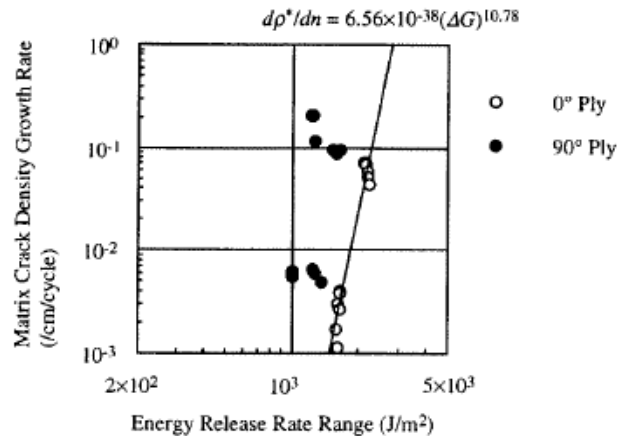

Figure 3.5 Crack density growth rate in thermal fatigue [7]

A decisive conclusion why the Paris law sometimes works and sometimes does not can not be given but the data subjected to analysis by this law have to be reconsidered with a caution

1) It can be noticed from Fig. 3.1 and many similar figures that most of the cracks cover the whole specimen width. It is a strong indication of an unstable crack growth, which can not be described by Paris law. For thick plies it is more typical that the cracks cover the whole width of the specimen.
2) Some cracks in Fig. 3.1 are not covering the whole width not because the propagation is stable but because they stop when approaching another existing crack (see 0-layer in Fig. 3.1).
3) Sometimes the same crack changes its plane (the crack front stops and the crack grow further in a slightly different position. This phenomenon is known also in monotonic loading and it is caused by mesoscale heterogeneity of the material.
4) The growth of some cracks stops because they are too close to existing crack (see 0-ply)

These observation lead to simple but very important conclusion: **The damage state in fatigue tests is often initiation governed.** Models based on strain energy release rates for self-similar crack growth can not be used in this case.

A good example for this situation are the data presented in Fig. 3.3 In laminates with cracked layer thickness m=8 and 12 the cracks went through the specimen as soon as they initiated and the law (1) is not applicably. So, the damage accumulation is initiation governed. It is very probably that the initiation has to be characterized by strength type of criteria. Kobayashi [5] obtained a very good fit to thermal fatigue data when using a strength based damage accumulation law, see Fig. 3.6, which also is an indication that the initiation governs the damage state

$$\frac{dD}{dN} = B\left(\Delta\sigma_{2av}^{k}\right)^{\delta} \qquad (2)$$

Crack density growth rate with the average stress in the layer was the same for surface and for the inside layer.

$dp^{*}/dn = 8.45\times10^{-22}(\Delta\sigma^{k(a)})^{9.44}$
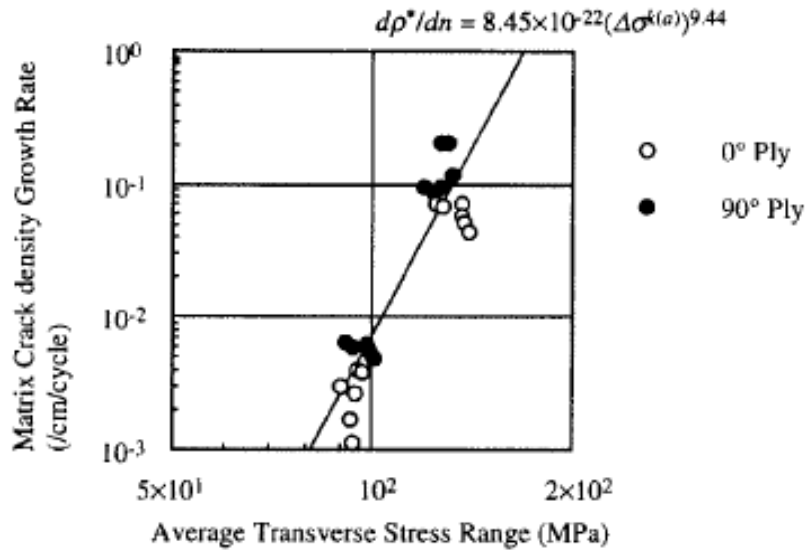
Figure 3.6 matrix crack density growth rate in thermal fatigue as a function of the average transverse stress change [2].

Takeda [4] analyzed transverse crack initiation in mechanical fatigue in T800H/3631 [0,90m,0] cross-ply laminates and came to conclusion that initiation is governed by following power law

$$\Delta\varepsilon N_{in}^{\alpha_{in}} = C_{in} \qquad (3)$$

Results in Fig. 3.7 confirm this hypothesis. According to (3) there is a power law relationship between the strain change in the cycle and the number of cycles to initiate the first crack.
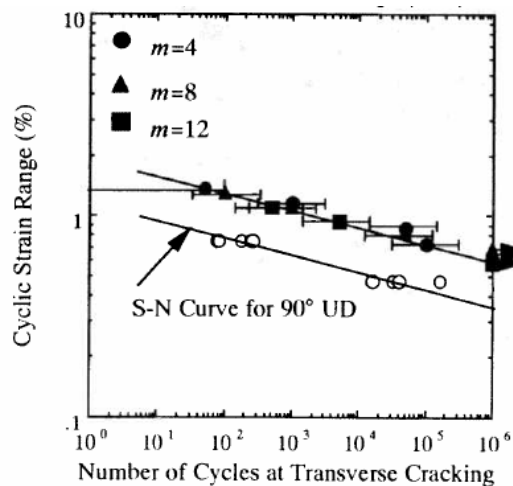
Figure 3.7 Relationship between the cyclic strain level and the number of cycles to initiate first transverse crack [4].

It is interesting to note that the slope of the curve in the log-log axes is the same as for the S_N curve for UD specimens in transverse tensile loading.

What was not recognized in [4] is the fact that actually many cracks are "first cracks" in the sense that the crack density is not reaching saturation. The different number of cycles required to initiate new cracks is related to the statistical distribution of microdefects in the material which evolves with the number of cycles.

Finally, measurements of local delamination growth at the transverse crack tip, see for example Takeda [4], have shown that the delamination growth is a stable process which can be reliable described by fracture mechanics.
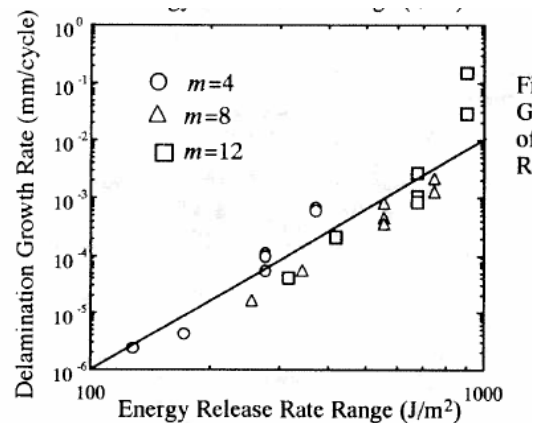
Figure 3.8 Local delamination growth rate as a function of energy release rate range [4].

As one can see Paris law is able to describe the local delamination .

3.2 Theoretical model to analyze the crack initiation

In this subsection a model is suggested to analyze crack initiation.

It is based on conclusion in the subsection 3.1 that the crack initiation is most probably strength governed. Since strength has statistical nature, the crack initiation also should be analyzed in terms of probability of initiation as a function of the stress state and the number of cycles. Certainly the micromechanical foundation of the initiation can still be defect state development with the number of cycles and the stress/strain level.

The approach can be briefly described as follows using the schematic representation in Fig. 3.9.


(edge view)
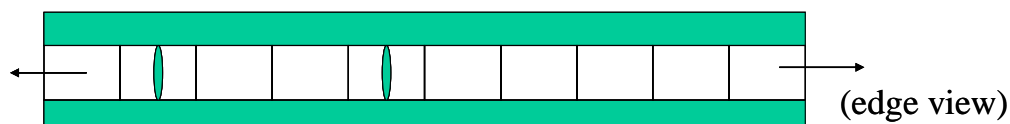
Figure 3.9 Schematic view of the specimen edge divided in small elements with statistical distribution of microdefects leading to variability of strength.

The procedure is the same for mechanical and for thermal loading

- Divide the layer which will have cracks (or the edge region of it if this is the initiation region because of stress state features) in M elements. The stress state is the same in all of them (non-interactive cracks). One element can contain only one crack
- Each element has its strength according to Weibull distribution
- With increasing applied stress and/or number of cycles first the weakest element will have a crack, than the next weakest etc

In order to simulate damage evolution we have to know defect size distribution which most probably depends on the number of experienced cycles N.

The representation in Fig. 9 is the same as in Weibull's weakest link theory. The edge of the layer is represented by a chain of elements linked together, with the element length ΔL_i approaching to zero.

The defect (flaw) size distribution in the material is characterized by n_σ -the number of flaws per unit length which may lead to failure at stress σ.

The probability of an element failure is proportional to its length and to n_σ. The probability of survival of the whole layer at a certain stress is

$$P_s = P_{s1}P_{s2}P_{s3}...P_{sM} = (1 - P_{f1})(1 - P_{f2})(1 - P_{f3})..(1 - P_{fM})$$ (4)

Which may be replaced by

$$P_s = 1 - \exp(-Ln_\sigma)$$ (5)

Weibull assumed that n_σ follows the power law with respect to the applied stress level which leads to

$$n_\sigma L_0 = \left(\frac{\sigma}{\sigma_0}\right)^m$$ (6)

We suggest the n_σ - the number of defects per unit length which can lead to crack at certain stress level, depends not only on the stress level but also on the number of cycles. In other words the defect state evolves with the number of cycles. Since no information is available about this dependence we describe it by a power law with respect to N. So, instead of (6) the following expression is suggested

$$n_\sigma L_0 = N^n \left(\frac{\sigma}{\sigma_0}\right)^m$$ (7)

which after substitution in (5) leads to the following expression for the probability of cracking in fatigue

$$P_s = 1 - \exp\left(-\frac{L}{L_0}N^n\left(\frac{\sigma}{\sigma_0}\right)^m\right)$$ (8)

For a certain fixed probability of failure of an element (it corresponds to a certain number of broken elements in Fig. 3.9) from (8) follows

$$const = N^n \left(\frac{\sigma}{\sigma_0} \right)^m \qquad\qquad\qquad (9)$$

This expression coincides in form with the expression (3) obtained in above described test.

Assuming that the distribution (8) is adequate, experimental data have to be gathered to determine the involved material constants n, m, σ_0.

Constants m and σ_o may be determined in a one-cycle monotonous loading test ($N = 1$)..
The procedure is as follows:

- use the multiple cracking data (crack density versus strain) for laminates with rather thick 90-layers where cracking is initiation governed and cracks grow in an unstable manner.
- Divide the strain region in the crack density- strain curve in zones and represent all the new cracking event in this zone by the average value of strain. Calculate the CLT stress in the layer corresponding to this average strain (including thermal stresses)
- Determine the relative number of new cracks corresponding to this zone represented by the calculated average stress in this layer. The relative number of new cracks is defined as the number of new cracks divided by the total number of elements (it is equal to the maximum possible number of cracks at saturation). Present the relative number of new cracks as the probability of failure at this stress level
- Find Weibull parameters in a standard fitting procedure in log-log axes.

Fatigue parameter n in the defect distribution function can be obtained from fatigue test at plotting the number of initiated cracks versus the number of cycles. The number of initiated cracks can be expressed through probability. Plotting the probability versus the number of cycles in double log-log axes we should according to the model obtain a linear relationship and the slope of it will give the parameter n.

If the model (8) is correct the slope has to be independent on the applied stress level in the fatigue test. Different stress levels would lead to vertical shift of curves. It has to be validated. Otherwise this parameter is a function of the stress level in the 90-layer, $n = n(\sigma)$.

4. Conclusions

This report contains new results concerning the local stress concentrations responsible for stitch crack formation in layers adjacent to layers containing intralaminar cracks. Analysis was performed using FEM.

The potential to improve the stress distribution (reduce stress concentrations) by changing the geometrical parameters of layers was not successful: the stress concentration shape was not changing significantly.

An introduction of an inter-layer with fiber orientation transverse to the fiber orientation in the layer with intralaminar cracks is a possible solution: a) stitch cracks in the inter-layer do not form because of the fiber orientation; b) the stress concentration is localized in the inter-layer only. This conclusion holds also for rather thin interlayer with a thickness = 0.25 of a regular prepreg layer thickness.

A statistical model for crack initiation in fatigue is suggested. It can be considered as a generalization of the Weibull's strength distribution model to fatigue case. Fatigue effects in the distribution are included by considering the defect distribution development with time and stress. Methodology for testing to validate the model and to determine the involved material parameters is described.

5. References

1. Bechel VT, Negilski, M. and J. James, Limiting the permeability of composites for cryogenic applications, Composites Science and Technology, 2006
2. S. Kobayashi S., Terada K., Ogihara Sh., Takeda N., Damage-mechanics analysis of matrix cracking in cross-ply CFRP laminates under thermal fatigue, Composites Sci & Techn. , 61, (2001); 1735-1742.
3. Nairn Nairn, J.and Hu, S., Matrix microcracking . In: Pipes R.B, Talreja R, ed. Comp. Mater. series, vol. 9. Dam. Mech. Comp. Mater. Amsterdam: Elsevier, (1994);187-243..
4. N. Takeda N., Ogihara Sh. And Kobayashi A. Microscopic fatigue damage progress in CFRP cross-ply laminates, , Composites, 26 (1995); 859-867.
5. Nairn J., "Fracture Mechanics of Composites with Residual Thermal Stresses," *J. Appl. Mech.,* 64, 804-810 (1997).
6. McManus H.L., Bowles D.E. and S.S. Tompkins, Prediction of thermal cycling induced matrix cracking, J. reinforced Plastics and Composites, 15, (1996); 124-140.

List of Figures